Hindawi
International Journal of Aerospace Engineering
Volume 2022, Article ID 8561245, 12 pages
https://doi.org/10.1155/2022/8561245

Research Article

Cooperative Search Optimization of an Unknown Dynamic Target Based on the Modified TPM

Kaixin Cheng,[1] **Di Wu**,[1] **Tao Hu**,[1] **Jinjin Wei**,[2] **and Zhifu Tian**[1]

[1]*College of Data Target Engineering, Strategic Support Force Information Engineering University, Zhengzhou 450001, China*
[2]*College of Information System Engineering, Strategic Support Force Information Engineering University, Zhengzhou 450001, China*

Correspondence should be addressed to Di Wu; wudipaper@sina.com

Received 31 October 2022; Revised 22 November 2022; Accepted 23 November 2022; Published 12 December 2022

Academic Editor: Xingling Shao

Aiming to address the problem of unknown dynamic target trajectory prediction and search path optimization in unmanned aerial vehicle (UAV) swarm path planning, this paper proposes a target search algorithm based on a modified target probability map (TPM). First, using the TPM, the proposed algorithm generates a high-probability distribution region of a target with directionality to fit the target trajectory and realizes the trajectory prediction of an unknown dynamic target. Then, the distributed ant colony (ACO) algorithm and the artificial potential field (APF) algorithm are combined to generate and optimize the UAV swarm search result and return path with the goal of maximizing task execution efficiency. Finally, the Monte Carlo simulation method is used to analyze the effectiveness of the proposed algorithm, and the results are evaluated from five aspects, including the number of targets captured. The simulation results show that under the condition of an unknown dynamic target trajectory, the average target captured rate and average unknown region search rate of the MTPM method were higher than that of the traditional TPM method, and the performance was improved by 14.6% and 10.7%, respectively.

1. Introduction

In an increasingly complex battlefield environment, reconnaissance and strike of targets in unknown battlefield areas are important means of war. Unmanned aerial vehicles (UAVs) play an increasingly important role in many fields, including reconnaissance, fire strikes, and electromagnetic interference, and can effectively reduce war losses and casualties. However, due to the limited load capacity and flight capacity of a single UAV, when performing large-scale combat missions, multiple UAVs have been commonly used to carry various types of sensors and loads to establish a wireless sensor network [1], which can improve the combat efficiency through cooperative mission planning between multiple UAVs. At present, much research has been conducted on multi-UAV cooperative task allocation and path planning, and good research results have been achieved [2–4].

In practical applications, the UAV path needs to be replanned frequently under the conditions of changing terrain data and dynamic target trajectories. However, the traditional exact solution algorithm has the problem of high time complexity, and the traditional heuristic algorithm has the problem of poor adaptability, which cannot quickly generate the optimal path [5]. Therefore, it is crucial to plan an efficient and reasonable search path for UAVs under the uncertain environments [6]. For this reason, it is necessary to solve the problem of dynamic target trajectory prediction and then to generate and optimize the search path. The parameter setting in the traditional TPM algorithm [7, 8] is not comprehensive enough to make full use of the target motion state data, so it cannot predict the target trajectory well. In addition, the traditional APF algorithm [9] is commonly used to deal with the obstacle avoidance problem but is easy to fall into a local optimum under an uncertain environment.

In this paper, we study the problem of multi-UAV cooperative mission path optimization for unknown dynamic targets. Aiming at this problem, this paper proposes a target search algorithm based on a modified target probability map (MTPM). First, the prediction model of unknown dynamic

targets is improved, and a directional two-dimensional normal probability distribution map is constructed to fit the target trajectory, realizing the trajectory prediction of unknown dynamic targets. Then, the UAV swarm search and return path with the maximized task execution efficiency are generated and optimized by a joint distributed ACO–APF algorithm. Finally, 30 batches of data are generated by the Monte Carlo method to simulate and analyze the efficiency of the proposed algorithm. The simulation results are evaluated from five aspects: the search rate of an unknown region, the search rate of TPM, the number of captured targets, the obstacle avoidance situation of UAV, and the target captured rate of 30 simulations. The experimental results verify that the proposed algorithm can solve the problems of trajectory prediction and search path optimization of unknown dynamic targets. Under the condition of an unknown dynamic target trajectory, the average target captured rate and average unknown region search rate of the MTPM method were higher than that of the traditional TPM method, and the performance was improved by 14.6% and 10.7%, respectively.

The main contributions of this paper can be summarized as follows:

(1) The prediction model of an unknown dynamic target is improved, and a directional two-dimensional normal probability distribution diagram is generated to fit the target trajectory

(2) The joint ACO–APF method is introduced to generate the artificial attractive potential field and the repulsive potential field based on the target trajectory prediction

(3) The state transition rules based on the ACO algorithm and MTPM method are designed to generate the optimal path of the UAV swarm search under the constraints of multiple systems

The rest of this paper is organized as follows. Section 2 describes the environment modeling method of UAV path planning. Section 3 introduces the proposed MTPM collaborative search path generation and optimization method. Section 4 presents the experimental simulations and compares the experimental results. Section 5 discusses open issues. Finally, Section 6 concludes the paper.

2. Related Work

In the research on the UAV cooperative mission path planning, considering the perspective of uncertainty, environments can be divided into deterministic environments and uncertain environments. In deterministic environments, the size, shape, and position of obstacles are known before planning, so no unknown dynamic changes in obstacle parameters and other environmental factors can occur. In contrast, in uncertain environments, obstacles and environmental factors are completely or partially unknown in a planning system, obstacles can suddenly appear or move, and there are dynamic disturbances in an environment [6].

The cooperative path planning method for multiple UAVs in a deterministic environment can be regarded as an NP-hard combinatorial optimization problem with many constraints [10]. In recent years, many scholars have conducted extensive research on how to establish mathematical models and solve the NP-hard combinatorial optimization problem [11–18]. The main mathematical models include the multitrip salesman model (MTSP), mixed linear integer programming model (MILP), and vehicle scheduling and path planning model (VRP). These models can be solved by heuristic algorithms, such as genetic algorithm (GA) [12], evolutionary algorithm (EA) [13, 14], ant colony (ACO) algorithm [15, 16], and particle swarm optimization (PSO) algorithm [17, 18].

Considering the problem of trajectory prediction of unknown dynamic targets, in reference [7], the authors established a rasterized environmental uncertainty map, search probability map, and pheromone map model and determined the prediction probability distribution of dynamic time-sensitive targets by calculating the target transition probability. Based on the target probability graph method, a linear model was developed to predict the location of unknown targets and solve the search problem of linear moving targets [8]. However, this method is not suitable for curved moving targets and cannot effectively solve the trajectory prediction problem of unknown dynamic targets.

Aiming at the generation and optimization of the search path, currently, the general research goal is to maximize the efficiency of task execution by effectively modeling the obstacle area [19, 20], and then, the artificial potential field (APF) method [9], the improved RRT* algorithm [21–24], and heuristic algorithms have been employed to generate an optimal path while solving spatial conflicts. The Circular Arc Trajectory method was used to model the irregular obstacle area, which could simplify the computational complexity of the obstacle avoidance problem [19]. The improved APF algorithm and a path optimization method for multiobstacle avoidance were proposed to solve the problem of path of UAV swarm falling into deadlock [20]. However, the method was not suitable for dynamic environments. The approaches abovementioned can solve the problems of irregular obstacle area modeling and obstacle avoidance path generation and optimization to a certain extent. However, under the condition of an unknown battlefield environment, there have still been a number of problems, such as an unreachable path, easy falling into a local optimum, and slow convergence speed. In conclusion, the abovementioned methods cannot effectively solve the problem of search path generation and optimization in an unknown battlefield environment.

3. Problem Description and Mathematical Model

Aiming at the problem of UAV group mission planning, the battlefield area is considered a two-dimensional area with a fixed height. The task content is as follows. Assume there are N_T unknown moving targets and N_O unknown obstacle areas in a battlefield area. N_{uav} fixed-wing UAVs with initial

flight resources of E_{uav} are sent to enter the unknown battlefield area to perform target reconnaissance and capture tasks. When the target reaches target R_{atk}, the target is determined to be captured, and the target stops moving. When the UAV swarm captures all targets or the flight resources are insufficient, the UAV swarm returns to the preset return point. After all UAVs return to the return point, the mission ends.

This section designs a UAV swarm mission planning system from three aspects: mission environment modeling, target modeling, and constraint modeling, and builds an environment for the search path optimization algorithm in the next section.

3.1. System Environment Modeling. Using the geometric graph method [25], the battlefield area can be rasterized into a set $\text{MAP} = \{(m, n) | m = 1, 2, \cdots, L_x, n = 1, 2, \cdots, L_y\}$, with a size of $L_x \times L_y$ corresponding to the cell in row m and column n.

The UAV track is connected by adjacent grid nodes. A UAV is defined as a fixed-wing UAV with a fixed speed V_{uav} cruise, a detection radius R_{uav}, and a target capture radius R_{atk}, having the maximum steering angle of $\varphi_{\max}$.

A set $\{X_{\text{uav}}, Y_{\text{uav}}, E_{\text{uav}}, \Theta_{\text{uav}}\}$ describes the UAV motion state, where X_{uav} and Y_{uav} represent the abscissa and ordinate of the current UAV position, respectively, E_{uav} is the current flight resource surplus of the UAV, and Θ_{uav} denoted the current motion direction of the UAV.

To facilitate research, this paper makes the following assumptions:

(i) UAVs can communicate with each other without considering the communication delay and communication distance, namely, a UAV can obtain information on other UAVs immediately

(ii) The flight resource consumption is not considered during the take-off and landing of a UAV

(iii) The UAV airborne processor's data processing time is not considered

3.2. Moving Target Modeling. First, the attributes and target trajectory of a target are modeled. It is assumed that a target T_i with coordinates $(X_T^{(i)}, Y_T^{(i)})$ moves periodically following the trajectory parameter equations given by

$$\begin{aligned} X_T^{(i)} &= R_{Tx}^{(i)} \cos\left[w_T^{(i)}\left(t_0^{(i)} + t\right)\right] + C_{Tx}^{(i)}, \\ Y_T^{(i)} &= R_{Ty}^{(i)} \sin\left[w_T^{(i)}\left(t_0^{(i)} + t\right)\right] + C_{Ty}^{(i)}, \end{aligned} \tag{1}$$

where $i \in \{1, \cdots, N_T\}$; set $(C_{Ty}^{(i)}, C_{Tx}^{(i)})$ represents the trajectory center coordinates; $R_{Tx}^{(i)}$ and $R_{Ty}^{(i)}$ represent trajectory equation's horizontal and vertical axis wheelbases, respectively; ω_T^i is the angular velocity of a target T_i moving on the trajectory; $t_0^{(i)}$ is the initial time of a target T_i motion; t denotes the current system time.

Set $\{X_T, Y_T, V_T, \Theta_T\}$ describes the motion state of targets, where X_T and Y_T represent the current abscissa and ordinate values of the target, respectively, V_T is the current velocity scalar of the target, and Θ_T denotes the current motion direction of the target.

3.3. System Constraint Modeling. Reference [18] proposed a circular overfitting method to establish an obstacle area model, which solved the problem of modeling and obstacle avoidance in irregular obstacle areas. According to the obstacle region modeling method based on a circular trajectory proposed in this paper, the obstacle region can be considered a circular region, and $(C_{Ox}^{(i)}, C_{Oy}^{(i)})$ and $R_O^{(i)}$ represent the center coordinates and radius of the Obstacle$_i$ region, respectively.

The following system constraints are defined:

$$\begin{aligned} &S_u : d_{uu}^{(ij)} \geq R_{\text{safe}}, \\ &S_o : d_{uo}^{(ij)} \geq R_{\text{safe}}, \\ &S_e : e_{\text{uav}}^{(i)}(k) \geq \lambda_E \min\left(d_{uE}^{(ij)}\right), \\ &S_p : \left\{ S_{op} | \varphi\left(\overrightarrow{s_{op}^{(j)} - s_{\text{uav}}^{(i)}}, \overrightarrow{\theta_{\text{uav}}^{(i)}}\right) \leq \varphi_{\max} \right\}, \end{aligned} \tag{2}$$

where S_u and S_o represent the distance constraint between UAVs and the distance constraint between UAVs and obstacle region, respectively, and they should be larger than the minimum threshold; S_e represents the UAV flight resource constraint, which needs to meet the minimum return flight resource threshold during the task execution process; S_p represent the UAV flight performance constraint, and the UAV yaw angle needs to be less than the maximum yaw angle threshold.

4. Search Path Generation and Optimization Algorithm

Aiming at the problem of unknown dynamic target trajectory prediction and search path optimization, based on the system modeling presented in the previous section, this section uses the MTPM method to generate a directional two-dimensional normal probability distribution map to fit the target trajectory and realize the trajectory prediction of unknown dynamic targets. The joint ACO–APF algorithm, where the APF algorithm is used to generate the MTPM attraction field, obstacle area repulsion field, and interaircraft repulsion field, is introduced. Combined with the state transition rules based on the ACO algorithm, the UAV swarm search and return path are generated and optimized under the premise of maximizing task execution efficiency.

4.1. Modified Target Probability Map. An unknown dynamic target refers to a target with uncertain coordinates, velocity, and direction of motion. To make full use of the limited known information to describe the distribution of unknown dynamic targets in the battlefield area, the target probability map method has usually been used to characterize the existence probability of the target at certain coordinates in the

battlefield area. However, due to the limitations on the parameter settings of the two-dimensional normal probability distribution model in the traditional algorithm, the traditional target probability map methods can describe the distribution only of unknown static targets and cannot solve the trajectory prediction problem of unknown dynamic targets.

To solve this problem, using the Pauta criterion and the two-dimensional normal probability distribution model, this paper maps the motion state of a target to the variance of the horizontal and vertical axes and generates a directional two-dimensional normal probability distribution map to fit the target motion trajectory and realize the trajectory prediction of unknown dynamic targets.

Define $p_i(m, n)$ as a distribution probability of a target T_i at coordinates (m, n) and assume that the motion state of target T_i can be detected as follows. Assume the detection coordinate is (m_0, n_0), the detection interval is τ_{scan}, the velocity is $v_T^{(i)}$, and the direction of motion is vector $\theta_T^{(i)}$. Based on the two-dimensional normal distribution model, the probability of the presence $p_i(m^*, n^*)$ of target T_i at coordinates of $(m^*, n^*) \sim N(m_0, n_0, \sigma_x^2, \sigma_y^2, \rho)$ is given by

$$p_i(m^*, n^*) = \frac{1}{2\pi\sigma_x^2\sigma_y^2\sqrt{1-\rho^2}} e^{-1/2\left(1-\rho^2\right)\left[(m^*-m_0)^2/2\sigma_x^2 - 2\rho(m^*-m_0)(n^*-n_0)/\sigma_x\sigma_y + (n^*-n_0)^2/2\sigma_y^2\right]}, \tag{3}$$

where a set $\{\sigma_x^2, \sigma_y^2, \rho\}$ refers to undetermine parameter groups, representing the horizontal axis variance, the vertical axis variance, and horizontal-vertical axes correlation coefficient; τ_{scan} represents the time needed for determining the target motion state; $\theta_T^{(i)}$ represents the angle between vector $\theta_T^{(i)}$ and the horizontal axis's positive direction.

It is assumed that the motion state of target T_i remains unchanged during the detection interval τ_{scan}, namely, target T_i moves from point $\text{A}(m_0, n_0)$ to point $\text{B}(m + \cos(\theta_T^{(i)})v_T^{(i)}\tau_{\text{scan}}, n + \sin(\theta_T^{(i)})v_T^{(i)}\tau_{\text{scan}})$ along the direction of $\theta_T^{(i)}$; its motion time is τ_{scan}, and its motion distance is $\delta_{\text{AB}}^{(i)} = v_T^{(i)}\tau_{\text{scan}}$. Substituting the motion state information of target T_i into the variance theorem yields to

$$\sigma_y = \tan^2\left(\theta_T^{(i)}\right)\sigma_x, \theta_T^{(i)} \in [-\pi, \pi). \tag{4}$$

After obtaining the mathematical relationship between variances along the horizontal and vertical axes, the next challenge is to increase the distribution probability of the projection of line segment AB in the model maximally so that the probability distribution model can fit the trajectory of target T_i and achieve the purpose of trajectory prediction. From the differential point of view, when the line segment AB is short enough, namely, when the detection frequency is high enough, continuous target detection can generate a continuous target trajectory.

To make the distribution probability of the projection of the motion trajectory in the model the highest and the trajectory the best fit, the Pauta criterion, namely the three-sigma criterion of normal distribution, is used in this study. Based on this criterion, a mathematical relationship between the variance of three times the motion trajectory and the motion distance $\delta_{\text{AB}}^{(i)}$ can be obtained as $\delta_{\text{AB}}^{(i)} = 3\sqrt{\sigma_x^2 + \sigma_y^2}$. Then, Equation (6) can be obtained as follows:

$$\begin{aligned} \sigma_x &= \frac{v_T\tau_{\text{scan}}}{3\sqrt{\tan^4\left(\theta_T^{(i)}\right) + 1}}, \\ \sigma_y &= \frac{\tan^2\left(\theta_T^{(i)}\right)v_T\tau_{\text{scan}}}{3\sqrt{\tan^4\left(\theta_T^{(i)}\right) + 1}}. \end{aligned} \tag{5}$$

According to the two-dimensional normal probability distribution theorem and Equation (6), the correlation matrix Φ can be obtained as follows:

$$\Phi = \begin{bmatrix} \left[\dfrac{v_T\tau_{\text{scan}}}{3\sqrt{\tan^4\left(\theta_T^{(i)}\right) + 1}}\right]^2 & \rho^{(i)}\left[\dfrac{\tan\left(\theta_T^{(i)}\right)v_T\tau_{\text{scan}}}{3\sqrt{\tan^4\left(\theta_T^{(i)}\right) + 1}}\right]^2 \\ \rho^{(i)}\left[\dfrac{\tan\left(\theta_T^{(i)}\right)v_T\tau_{\text{scan}}}{3\sqrt{\tan^4\left(\theta_T^{(i)}\right) + 1}}\right]^2 & \left[\dfrac{\tan^2\left(\theta_T^{(i)}\right)v_T\tau_{\text{scan}}}{3\sqrt{\tan^4\left(\theta_T^{(i)}\right) + 1}}\right]^2 \end{bmatrix}, \rho \in [-1, 1], \tag{6}$$

where parameter $\rho^{(i)}$ describes the linear correlation between the horizontal and vertical coordinates, and when $\theta_T^{(i)} \in \{[0, \pi/2] \cap [-\pi, -\pi/2]\}$, $\rho^{(i)}$ is positive; otherwise, it is negative.

Based on the abovementioned method and the motion state information of multiple targets, multiple directed two-dimensional normal probability distribution models can be generated to fit the transient motion trajectories of multiple targets. Using the normalization method, the target motion state information is brought into the calculation to generate the multitarget probability distribution matrix P_{MTPM} with a size of $L_X \times L_Y$, which can reflect the distribution probability of multitarget in the battlefield area; matrix P_{MTPM} is defined by

$$P_{\text{MTPM}} = \begin{pmatrix} p_{(1,1)} & \cdots & p_{(1,L_y)} \\ \vdots & \ddots & \vdots \\ p_{(L_x,1)} & \cdots & p_{(L_x,L_y)} \end{pmatrix}. \tag{7}$$

System initialization and iterative update of matrix P_{MTPM} are performed as follows.

Before a task starts, the motion state of an unknown moving target is detected N_{scan} times, the detection interval is τ_{scan}, and the initialization $P_{\text{MTPM}}^{(k=0)}$ is performed. During the mission execution process, matrix $P_{\text{MTPM}}^{(k)}$ is updated through a multi-UAV cooperative search with a search cycle of τ_k.

4.2. Path Generation and Optimization. The traditional ACO algorithm uses the initialization information for heuristic search through the positive feedback mechanism, which has the advantages of skipping a local optimal solution and approaching the global optimal solution. However, there are also problems of slow convergence and dependence on initialization information, which are specific to carpet search scenarios. The traditional APF algorithm can rapidly generate a direct path through the repulsion attraction mechanism and is suitable for searching for and approaching known targets and rapid escapes from obstacle areas, but there are problems, such as easy falling into a local optimum and unreachable generation path.

Combining the two aforementioned algorithms and using the initialization information of matrix $P_{\mathrm{MTPM}}^{(k=0)}$, a path generation algorithm, which can rapidly generate paths, avoid unreachable paths, and solve the above problems effectively, can be developed. The specific combined method is as follows. When the APF information is strong, the APF method is used to approach targets or escape from obstacles; otherwise, the ACO heuristic transfer method is used to generate an optimal search path.

4.2.1. Pheromone Map and APF Modeling. First, a pheromone matrix Aco with a size of $L_X \times L_Y$ is constructed to describe the current battlefield area search as follows:

$$\mathrm{Aco} = \begin{pmatrix} \mathrm{aco}_{(1,1)} & \cdots & \mathrm{aco}_{(1,L_y)} \\ \vdots & \ddots & \vdots \\ \mathrm{aco}_{(L_x,1)} & \cdots & \mathrm{aco}_{(L_x,L_y)} \end{pmatrix}, \mathrm{aco}_{(m,n)} \in [\mathrm{aco}_{\min}, \mathrm{aco}_{\max}], \tag{8}$$

where $\mathrm{aco}_{(m,n)}$ represents the pheromone value of a position (m, n); the higher the pheromone value is, the higher the search value of the position will be.

System initialization and iterative update are performed on the matrix Aco as follows. Before the task starts, the pheromone matrix value is initialized to $(\mathrm{aco}_{\min} + \mathrm{aco}_{\max})/2$. During the mission, the global pheromone increases with the system iteration number with an increment of $\mathrm{Aco}_{\mathrm{rise}}/\tau_k$, and UAVs cooperatively detect the pheromone value within the update distance. The update formula is given by

$$\begin{aligned} &\left\{ s_{\mathrm{aco}}^{(j)} \middle| \sqrt{\left[x_{\mathrm{uav}}^{(i)}(k) - a\right]^2 + \left[y_{\mathrm{uav}}^{(i)}(k) - b\right]^2} \le R_{\mathrm{uav}} \right\} \\ &d_{ua}^{(ij)} = \sqrt{\left[x_{\mathrm{uav}}^{(i)}(k) - a\right]^2 + \left[y_{\mathrm{uav}}^{(i)}(k) - b\right]^2}, \\ &\mathrm{Aco}(a,b) = \left[1 - \lambda_{\mathrm{Aco}}\left(1 - \frac{d_{ua}^{(ij)4}}{R_{\mathrm{uav}}^4}\right)\right]\mathrm{Aco}(a,b) \end{aligned} \tag{9}$$

where λ_{Aco} represents the pheromone elimination coefficient. Then, by using the APF algorithm, the repulsion potential field of the UAV is constructed with an obstacle area and a UAV as a center, and the collision avoidance paths between the UAV and the obstacle area and adjacent aircraft are generated. The attraction potential field of the UAV is centered on the target and the return point, and the approach search and return path of the UAV are generated.

Next, set the farthest distance of the repulsive potential field to R_{rep}, the minimum safe distance around a drone is R_{safe}, the modulus of the repulsive potential field force is $|\mathrm{Fu}^{(ij)}|, |\mathrm{Fo}^{(ij)}| \in [(R_{\mathrm{safe}}/R_{\mathrm{rep}})^2, 1]$, and it is negatively correlated with the distance; then, the resultant repulsive force is obtained by

$$\begin{aligned} \mathrm{Frep}_x^{(i)} &= \sum_{j=1}^{N_O} \mathrm{Fo}_x^{(ij)} + \sum_{j=1}^{N_T} \mathrm{Fu}_x^{(ij)}, \\ \mathrm{Frep}_y^{(i)} &= \sum_{j=1}^{N_O} \mathrm{Fo}_y^{(ij)} + \sum_{j=1}^{N_T} \mathrm{Fu}_y^{(ij)}, \end{aligned} \tag{10}$$

where $\mathrm{Frep}_x^{(i)}$ and $\mathrm{Frep}_y^{(i)}$ represent the transverse and longitudinal components of the resultant repulsive force; $\mathrm{Fu}_x^{(ij)}$ and $\mathrm{Fu}_y^{(ij)}$ denote the transverse and longitudinal components of the repulsive force $\mathrm{Fu}^{(ij)}$ between UAV_i and UAV_j; $\mathrm{Fo}_x^{(ij)}$ and $\mathrm{Fo}_y^{(ij)}$ are the transverse and longitudinal components of the repulsive force $\mathrm{Fo}^{(ij)}$ between UAV_i and $\mathrm{Obstacle}_j$

The farthest action distance of the target attraction potential field is R_{uav}, indicating that when the drone detects the target, the target can attract the drone, and the attraction mode is given by $|\mathrm{Fatt}^{(ij)}| \in [(R_{\mathrm{atk}}/R_{\mathrm{uav}})^2, 1]$.

Then, set the action distance of the return point attraction potential field to be unlimited; the return attraction is a unit vector, and the potential field action condition is given by $e_{\mathrm{uav}}^{(i)}(k) \le \lambda_E \min(d_{uE}^{(ij)})$, where $e_{\mathrm{uav}}^{(i)}$ represents the current flight resource surplus of UAV_i, $d_{uE}^{(ij)}$ is the distance from UAV_i to the return point j, and λ_E is the return parameter. If the condition is judged to be true, then the UAV flight resources are insufficient and need to return immediately; parameter λ_E is used to adjust the UAV return time point.

When a drone is affected by multiple attraction potential fields at the same time, only the attraction potential field force with the maximum modulus is retained; namely, the drone can be subjected to the attraction potential field force only in one direction at a time, as given by

$$\mathrm{Fatt}^{(i)} = \mathrm{Fatt}\left(\arg\max_{(j)} \left|\mathrm{Fatt}^{(i,j)}\right|\right), \tag{11}$$

where $\mathrm{Fatt}^{(ij)}$ represents the attraction vector of the target pair, $\arg\max_{(j)}|\mathrm{Fatt}^{(ij)}|$ is the attraction potential field force number with the largest modulus, and $\mathrm{Fatt}^{(i)}$ denotes the current attraction vector.

In summary, the generation formula of the artificial potential force $F^{(i)}$ of UAV_i at position $(x_{\mathrm{uav}}^{(i)}, y_{\mathrm{uav}}^{(i)})$ is defined by

$$\begin{aligned} F_x^{(i)} &= \mathrm{Frep}_x^{(i)} + \mathrm{Fatt}_x^{(i)}, \\ F_y^{(i)} &= \mathrm{Frep}_y^{(i)} + \mathrm{Fatt}_y^{(i)}. \end{aligned} \tag{12}$$

4.2.2. Route Generation Algorithm. The optimal decision-making method based on a battlefield environment of a UAV is as follows.

When APF information is strong, the APF method is used to approach targets or escape from obstacles; otherwise, the ACO heuristic transfer method is used to determine an optimal search path according to the target probability graph matrix and the pheromone matrix.

First, an optional grid set S_{op} can be obtained based on the flight performance constraint set $S_{\mathbf{p}} : \{S_{\mathrm{op}} | \varphi(\overrightarrow{s_{\mathrm{op}}^{(j)} - s_{\mathrm{uav}}^{(i)}}, \overrightarrow{\theta_{\mathrm{uav}}^{(i)}}) \le \varphi_{\max}\}$ by Equation (3), where $s_{op}^{(j)}$ represents the coordinates of the optional grid j; $s_{\mathrm{uav}}^{(i)}$ and $\theta_{\mathrm{uav}}^{(i)}$ denote the current coordinates and motion direction of UAV_i; $\varphi(x, y)$ is the angle between the two vectors. Then, the optimal path grid number j_{best} is obtained according to the optimal decision method; namely, $s_{\mathrm{op}}^{(j_{\mathrm{best}})}$ is the next transfer coordinate of UAV_i.

When $|\overrightarrow{F^{(i)}}| \neq 0$, that is, when the APF information exists, the APF method is used to generate the optimal search path. The grid in S_{op} with the smallest angle with vector $F^{(i)}$ represents an optimal grid, and it is given by

$$j_{\mathrm{best}} = \arg\min_{(j)} \left[\varphi\left(\overrightarrow{s_{\mathrm{op}}^{(j)} - s_{\mathrm{uav}}^{(i)}}, \overrightarrow{F^{(i)}} \right) \right]. \tag{13}$$

When $|\overrightarrow{F^{(i)}}| = 0$, that is, when the APF information does not exist, the ACO heuristic transfer method is used to generate an optimal search path. The target probability graph matrix $P_{\mathrm{MTPM}}^{(k)}$ and pheromone matrix $\mathrm{Aco}(k)$ are substituted into the ACO algorithm transfer probability formula, and the Bayesian probability $p_i^{(j)}(k)$ of $s_{\mathrm{op}}^{(j)}$ is calculated. Then, the roulette algorithm is used to generate an optimal grid as follows:

$$p_i^{(j)}(k) = \frac{\left[P_{\mathrm{MTPM}}^{(k)}(n, m)^{(ij)} \right]^{\alpha} \times \left[\mathrm{Aco}(k)(n, m)^{(ij)} \right]^{\beta}}{\sum_{s_o^{(j)} \in \mathbf{S}_{\mathrm{op}}} \left[P_{\mathrm{MTPM}}^{(k)}(n, m)^{(ij)} \right]^{\alpha} \times \left[\mathrm{Aco}(k)(n, m)^{(ij)} \right]^{\beta}}, \tag{14}$$

where parameter α is a heuristic factor, which represents the relative importance of the target probability distribution matrix $P_{\mathrm{MTPM}}^{(k)}$, and parameter β is a pheromone factor, which represents the relative importance of pheromone matrix $\mathrm{Aco}(k)$.

4.2.3. System Iterative Update. After obtaining the optimal grid number j_{best}, $s_{\mathrm{op}}^{(j_{\mathrm{best}})}$ represents the next grid coordinates of a UAV, the UAV path is generated, and the system is iteratively updated. The updating process is as follows. Update a UAV's position $s_{\mathrm{uav}}^{(i)}(k+1)$, flight resource surplus $e_{\mathrm{uav}}^{(i)}(k+1)$, and motion direction $\theta_{\mathrm{uav}}^{(i)}(k+1)$ as follows:

$$\begin{aligned} s_{\mathrm{uav}}^{(i)}(k+1) &= s_{\mathrm{op}}^{(j_{\mathrm{best}})}(k) \\ e_{\mathrm{uav}}^{(i)}(k+1) &= e_{\mathrm{uav}}^{(i)}(k) - d\left[s_{\mathrm{uav}}^{(i)}(k), s_{\mathrm{op}}^{(j_{\mathrm{best}})}(k) \right]. \\ \theta_{\mathrm{uav}}^{(i)}(k+1) &= \theta\left[\overrightarrow{s_{\mathrm{op}}^{(j_{\mathrm{best}})}(k)} - \overrightarrow{s_{\mathrm{uav}}^{(i)}(k)} \right] \end{aligned} \tag{15}$$

The algorithm flow of the path generation and optimization method based on the improved target probability graph is shown in Figure 1.

5. Simulation Experiments

This section presents the numerical simulation results of collaborative search tasks in uncertain dynamic environments. In the simulations, it was assumed that there were N_T unknown moving targets and N_O unknown obstacle areas in the battlefield area of a fixed height; N_{uav} fixed-wing UAVs with the initial flight resources E_{uav} were dispatched to perform reconnaissance and capture tasks. A target was judged to be captured when the distance between the UAV and the target was less than R_{atk}, and then, the target stopped moving. When the UAV captured all targets or flight resources were insufficient, the UAV returned to the preset return point. After all UAVs returned to the return point, the mission ended.

5.1. Parameter Settings. The mission of a UAV group was as follows. It was assumed that 20 patrol vehicles (unknown dynamic targets) patrolled at a constant speed around a certain point in a mission area. Then, four UAVs, which took off from the airports located at the four vertices of the mission area map, were dispatched to enter the mission area and perform a search and capture patrol vehicle mission. To improve the search efficiency of a UAV, the patrol vehicle was detected at intervals of τ_{scan} before the UAV swarm entered the task area, and the detection results were imported into the UAV swarm path planning system as a prior information. There were multiple unknown no-fly zones (unknown obstacle zones) in the mission area, and the minimum safe distance R_{safe} between the UAV group and the no-fly zone had to be maintained.

The battlefield area size was 200 km × 200 km, and it was rasterized into 1,000 grid × 1,000 grid, so 1 grid = 0.2 km. The UAV path defined the system iteration step size to be $\tau_k = 5$ s, and the system clock was $t_k = \tau_k \times (k-1)$. The simulation parameters are given in Table 1.

The Monte Carlo method was under the condition that the intersection of the target motion trajectory, and the obstacle area was empty. To mobilize the UAV group fully to perform a wide search of the task area, the special

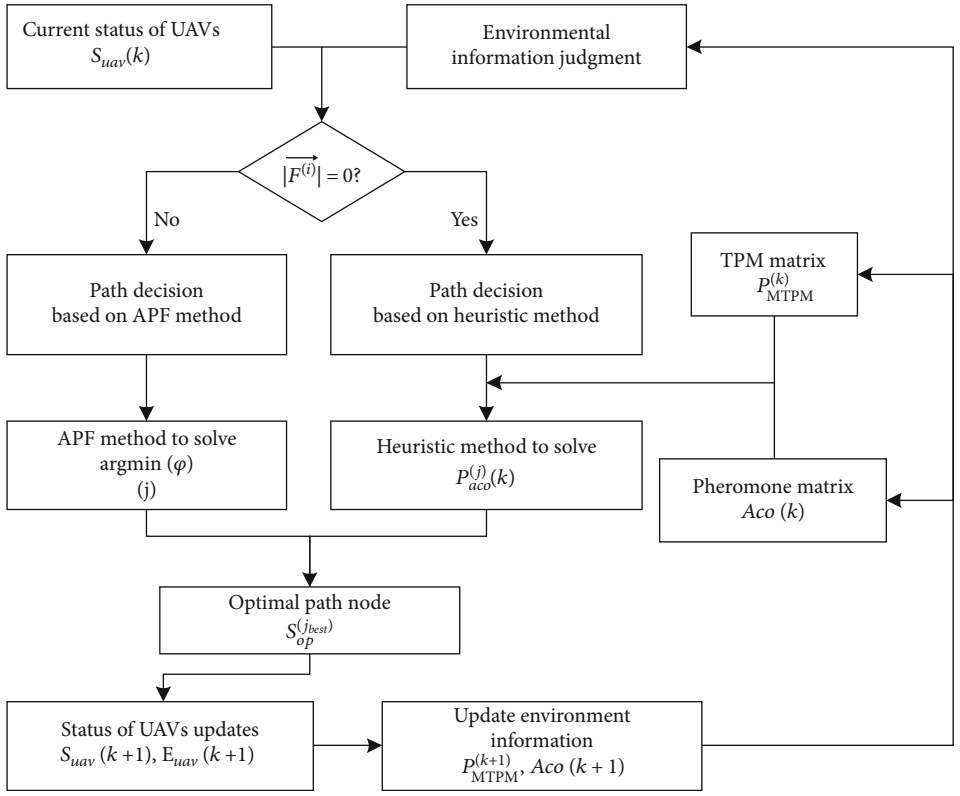

Figure 1: The block diagram of the proposed path generation and optimization method based on the MTPM.

situation of the target trajectory concentration should be avoided as much as possible. Therefore, according to the two-dimensional uniform distribution, multiple batches of relevant parameters were generated. Each batch contained 10 moving targets and 20 obstacle areas. The relevant parameters included the trajectory center of a moving target, long-axis wheelbase, short-axis wheelbase, the angular velocity of motion, the initial phase of motion, motion direction (clockwise or counterclockwise), and center and radius of the obstacle area. The ranges of parameters were set as presented in Table 2.

The Monte Carlo method was used to generate 30 batches of experimental data, and the experimental results were described and compared. The distribution of unknown dynamic target trajectory and obstacle area is shown in Figure 2. As shown in Figure 2, 10 moving targets and 20 obstacle areas were evenly distributed in the task area. The moving target moved in a periodic closed-loop around the center of the trajectory as shown in the blue curve, and the obstacle areas overlapped, forming an irregular obstacle area as shown in the black area. There was no intersection between the moving target trajectory and the obstacle area to avoid the situation of a drone entering the obstacle area to search for a target.

5.2. Experimental Results and Analysis. Aiming at the problem of unknown dynamic target trajectory prediction and search path optimization, the traditional TPM method is compared. The simulation results are shown in Figures 3 and 4, where the initial distribution of target probability ($k = 0$) and the cooperative search path are presented, respectively. Then, the effectiveness of the proposed method in an uncertain dynamic environment was evaluated using several evaluation indices, which included the search rate of an unknown region, the search rate of a target probability distribution, the obstacle avoidance of UAV, the number of captured targets, the number of captured targets in 30 times' simulations, and the unknown region search rate in 30 times' simulations, shown in Figures 5–8, respectively. The task execution efficiency was comprehensively evaluated in comparison with the traditional TPM method.

After importing the prior information into the system, the initial target probability distribution matrix $P^{(k=0)}_{\mathrm{TPM}}$ was generated using the proposed MTPM method and the traditional TPM method, as shown in Figure 3.

The initial distribution of target probability reflected a target's movement in the task area at the beginning of the task. The higher the target probability was, the more likely the target was to move around the position. In Figures 3(a) and 3(b), the results of the MTPM method are presented. In Figures 3(c) and 3(d), the results of the TPM method are illustrated. Figures 3(a) and 3(c) show the 3D images, and Figures 3(b) and 3(d) display the 2D images. Further, in Figures 3(c) and 3(d), the high-probability area of the target in the distribution map obtained by the traditional TPM method is dotted. Compared with the real motion trajectory of the target presented in Figure 2, the high-probability area of the target is discontinuous and has poor directivity, which cannot predict the target

Table 1: Simulation parameters.

Parameter	Simulated value	Actual value
Detection range R_{uav}	50 grid	10 km
Catching range R_{atk}	5 grid	1 km
UAV speed V_{uav}	$\left[1, \sqrt{2}\right]$ grid/τ_k	(144,200) km/h
Flight resources E_{uav}	2,400 grid	480 km
Safety distance R_{safe}	4 grid	0.8 km
Repulsive force distance R_{rep}	10 grid	2 km
System step length τ_k	1 step	5 s
Sampling period τ_{scan}	120 step	600 s

Table 2: Target and obstacle area parameters.

Parameter	Simulation value range	Actual value range
Target trajectory radius R_T	(20,50) grid	(4, 10) km
Target moving speed V_T	(0.4, 0.7) grid/τ_k	(57,100) km/h
Obstacle area radius R_O	(20,50) grid	(4, 10) km

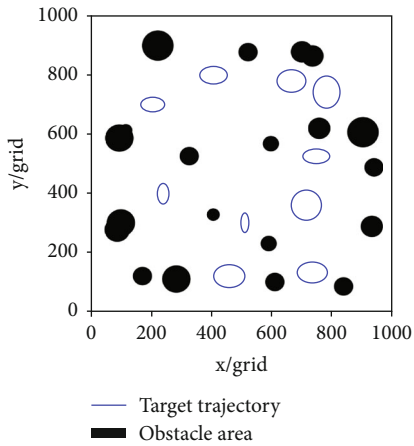

Figure 2: Unknown dynamic target trajectory and obstacle area distribution graph.

trajectory. Further, as shown in Figures 3(a) and 3(b), the distribution map obtained by the MTPM method showed a banded distribution of the high-probability region of the target. Compared with the actual motion trajectory of the target, which is displayed in Figure 2, the trajectory presented in Figure 3 could accurately reflect the motion trend and process of the target, indicating that the proposed MTPM method is more suitable for the motion trajectory prediction and fitting of the curve trajectory target than the traditional TPM method.

After the mission began, the UAV planned the search path according to the initial distribution of the target probability and reduced the target probability value of the explored area as the system iterated, updating the target probability distribution map. Figures 4(a) and 4(b) show the drone's search path. Figure 4(a) shows the results of the MTPM method. Further, Figure 4(b) shows the results of the traditional TPM method.

As shown in Figure 4(a), under the combined action of the distributed ACO algorithm and the APF algorithm, after the UAV effectively searched the high-probability area of the target, it captured all targets and successfully returned to the predefined return point, and the system iterations ended at $k = 1639$. The results in Figure 4(b) demonstrate that the UAV searched the high-probability area of the target, but due to the lack of effective target trajectory prediction, the drown cannot capture all targets, and the system iteration was ended at $k = 1686$. The comparison of the results showed that the initial distribution of the target probability generated by the MTPM method could accurately describe the motion trend of an unknown target. The joint distributed ACO–APF algorithm could correctly guide the UAV to search the high-probability area of the target effectively and jump out of the path deadlock.

The unknown area search rate and the target probability distribution search rate were calculated by Equations (16) and (17).

$$r_{cov}(k) = S_{cov}(k)/S_{L_x \times L_y}, \tag{16}$$

$$r_{TPM}(k) = 1 - \left[\frac{\sum_{b=1}^{L_y}\sum_{a=1}^{L_x} P_{TPM}^{(k)}(a,b)}{\sum_{b=1}^{L_y}\sum_{a=1}^{L_x} P_{TPM}^{(k=0)}(a,b)}\right]. \tag{17}$$

Figure 5(a) reflects the comparison of the two methods on the unknown region search rate which reflects the extent of the drone's search for unknown region, and Figure 5(b) reflects the comparison of the two methods on the TPM search rate which reflects the extent of the drone's search for the high-probability distribution region of targets. With the iteration of the system, the drone's search for unknown region gradually deepens based on the TPM matrix. In Figure 5, the end point represents the number of system iterations at the end of the task.

Figure 6 reflects the comparison of the two methods on the number of target capture which reflects the task efficiency of the drone. With the iteration of the system, the drone continuously discovers and captures the targets when searching the unknown region. In Figure 6, the end point represents the number of system iterations at the end of the task.

As shown in Figures 5 and 6, the MTPM method completed the iteration process at $k = 1639$, achieving a search rate of an unknown region of 44.7%, a search rate of the target probability distribution of 97.3%, and the number of captured targets of 10, which were better than those of the traditional TPM method. The three mentioned metrics of the traditional TPM method were 41.4%, 88.5%, and 9 at $k = 1686$, indicating that the effective trajectory prediction of the moving target by the MTPM method could accurately guide a UAV to search the path planning and achieve a better task execution effect.

Figure 7 reflects the comparison of the two methods on the distance to obstacle which reflects the obstacle avoidance

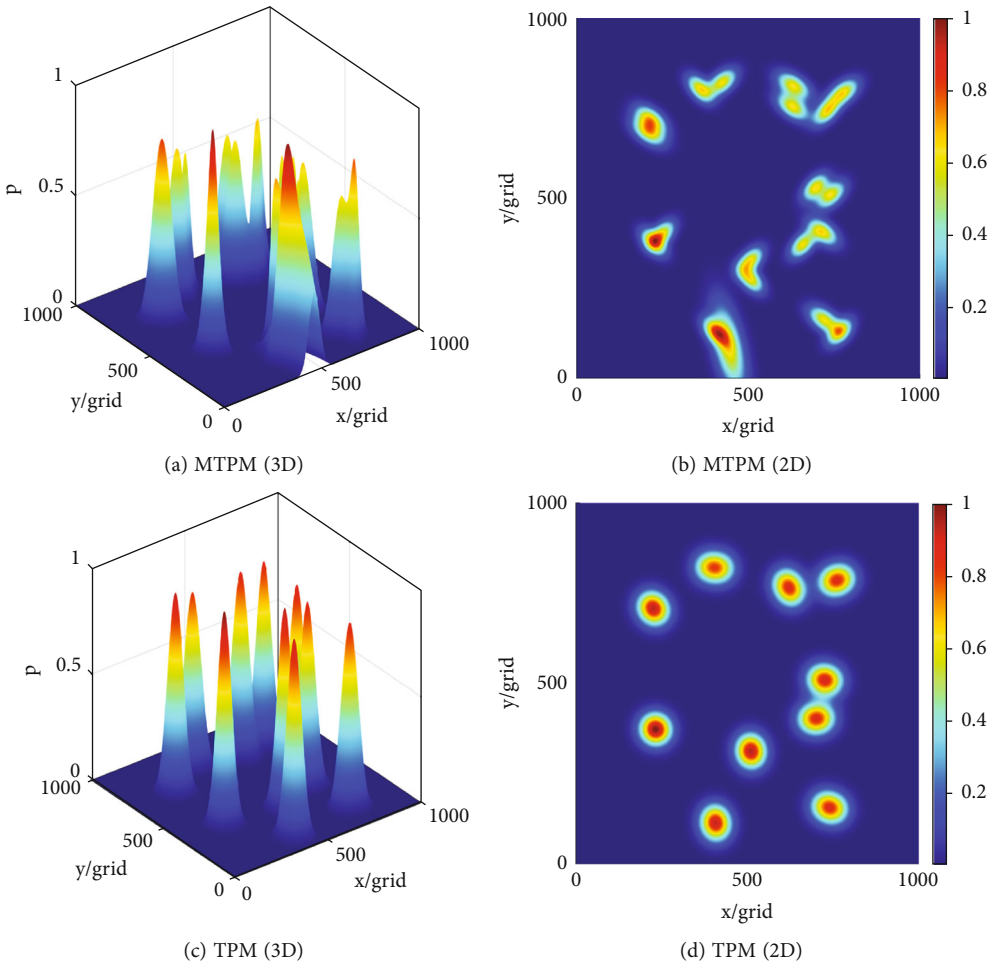

Figure 3: The initial distribution of target probabilities ($k = 0$).

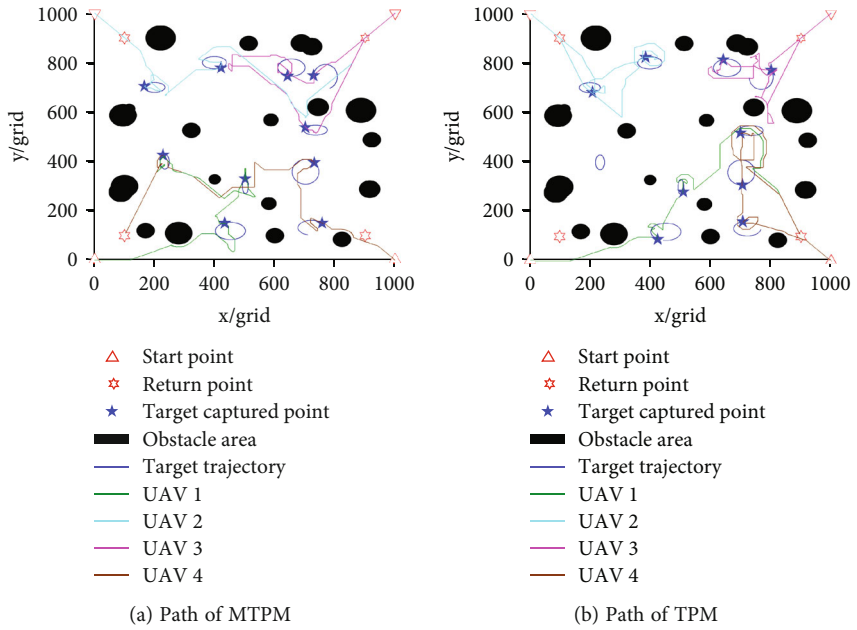

Figure 4: The cooperative search results.

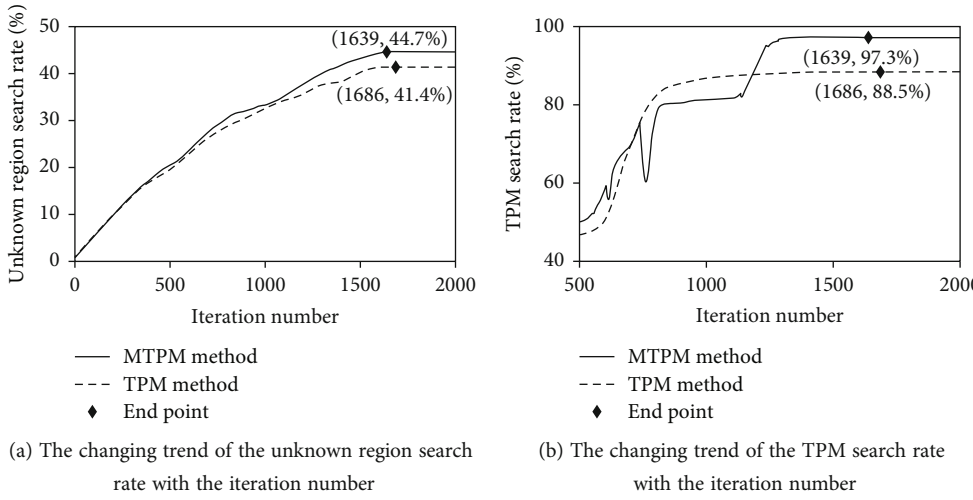

(a) The changing trend of the unknown region search rate with the iteration number

(b) The changing trend of the TPM search rate with the iteration number

Figure 5: Comparison on the search rate with the iteration number between the two methods.

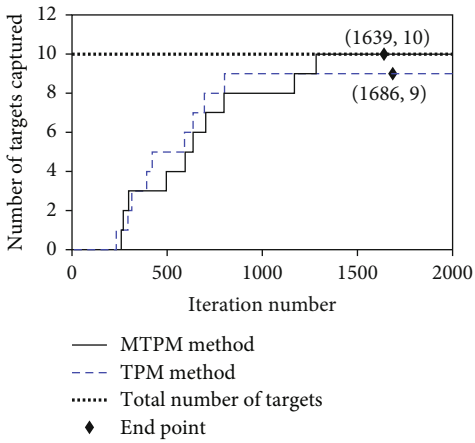

Figure 6: Comparison on the number of captured targets with the iteration number between the two methods.

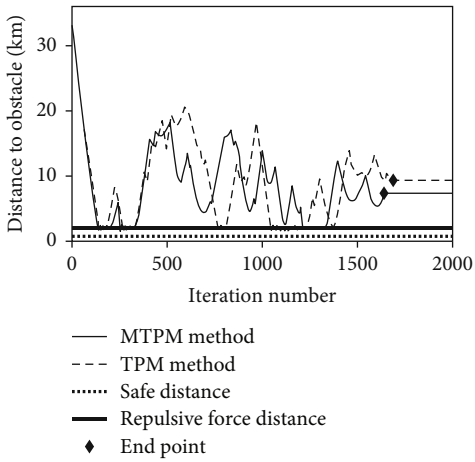

Figure 7: Comparison on the UAV obstacle avoidance result between the two methods.

situation of the drone. The vertical axis in Figure 5 represents the minimum distance from the drone to the obstacle area. The black solid line that changes with time corresponds to the data of the MTPM method, and the black dotted line corresponds to the data of the TPM method. The constant bold black solid line represents the maximum repulsive force distance R_{rep}(R_{rep} = 2km) in the APF algorithm. If the distance from the UAV to the obstacle area exceeds R_{rep}, the repulsive force from the obstacle area would be no longer applied to the UAV. The constant bold black dotted line represents the safety distance R_{safe}(R_{safe} = 0.8km) of the UAV in the APF algorithm. If the distance from the UAV to the obstacle area is less than R_{safe}, a collision would be happened between the UAV and the obstacle area.

As shown in Figure 7, the minimum distance between the UAV and the obstacle area is always longer than the safe distance R_{safe}, which shows that the obstacle repulsion potential field can avoid collisions between the UAV and the obstacle area. The reason is that the modulus of the repulsive force is inversely proportional to the square of the distance, so that the UAV can avoid obstacles at the right time and position.

Figure 8 reflects the comparison results in 30 simulations of the two methods. In Figure 8, the black color corresponds to the data of the MTPM method, and the blue color corresponds to the data of the TPM method.

In Figure 8(a), the vertical axis represents the number of targets captured by the drone. The dotted lines represent to the number of captured targets in 30 simulations, and the solid lines represent to the average number of captured targets in 30 simulations. After the subsimulation, the average number of captured targets of the MTPM method was 9.63, and the average number of captured targets of the TPM method was 8.4.

In Figure 8(b), the vertical axis represents the unknown region search rate. The dotted lines represent to the unknown region search rate in 30 simulations, and the solid lines represent to the average unknown region search rate in 30 simulations. After the subsimulation, the average

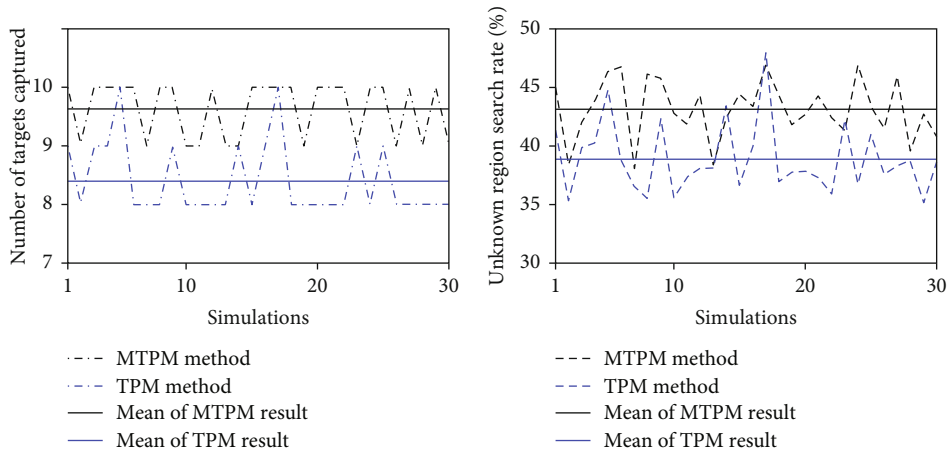

(a) Comparison results of targets captured in 30 simulations between the two methods

(b) Comparison results of unknown region search rate in 30 simulations between the two methods

Figure 8: Comparison results in 30 simulations between the two methods.

unknown region search rate of the MTPM method was 43.3%, and the average unknown region search rate of the TPM method was 39.1%.

According to the above-presented evaluation results, after the subsimulation, the average target captured rate and average unknown region search rate of the MTPM method were higher than that of the traditional TPM method, and the performance was improved by 14.6% and 10.7%, respectively, indicating that the traditional TPM method is deficient in trajectory prediction of dynamic targets. In contrast, the proposed method could effectively solve the search path optimization problem of unknown dynamic targets.

6. Conclusion

Under the condition of an uncertain dynamic environment, this paper studies the cooperative search problem of UAV swarm. In this study, an uncertain dynamic environment is defined as an unknown region, including the multiobstacle region and dynamic target with the periodic motion of curve trajectory. In addition, a cooperative search algorithm for UAVs based on the MTPM is proposed. From the aspect of prior information processing of a battlefield environment, aiming at improving the TPM method and making full use of limited target motion state information, a directional target probability distribution map is constructed and used to predict the target motion trajectory. To generate a UAV swarm's path, this paper combines the distributed ACO algorithm and the APF algorithm to develop the path generation method according to environmental information under the multisystem constraint. When the target information is sufficient, the APF method is used to obtain the target trajectory attraction potential field and the capture path. However, when the target information is insufficient, the ACO algorithm is combined with the MTPM method into a heuristic ACO-based probability transfer method, which is used to determine a search path. After the mission ends, the UAV can return to the predefined return point. Finally, the Monte Carlo method is used to perform simulation experiments, and five indicators are used for evaluation, namely, the unknown region search rate, the TPM search rate variations, the number of captured targets, the UAV obstacle avoidance result, and the comparison results of targets captured in 30 simulations using different methods. The experimental results verify that the proposed search path planning method based on the improved target probability graph can achieve high efficiency under the condition of limited target motion information. The average target captured rate and average unknown region search rate of the MTPM method were higher than that of the traditional TPM method, and the performance was improved by 14.6% and 10.7%, respectively, indicating that the proposed algorithm can effectively solve the problem of UAV cooperative search task planning in uncertain dynamic environments. At present, there are some shortcomings in the design method of the UAV flight model. We are reading relevant literature on the mobile robots and quadrotors control algorithm [26–30], hoping to improve our work by combining these technologies in the next step. Future research will focus on how to improve the UAV flight model and smooth its path. In addition, a new UAV swam path planning algorithm will be designed for the improved UAV flight model to generate a better multi-UAV cooperative search path that can better meet actual needs.

Data Availability

The data used in this study have been mainly obtained in the simulation experiments.

Conflicts of Interest

The authors declare that they have no conflicts of interest.

Acknowledgments

This work was supported in part by the National Natural Science Foundation of China under grant no. 42201472.

References

[1] R. Shakeri, M. A. Al-Garadi, A. Badawy et al., "Design challenges of multi-UAV systems in cyber-physical applications: a comprehensive survey and future directions," *IEEE Communications Surveys & Tutorials*, vol. 21, no. 4, pp. 3340–3385, 2019.

[2] G. W. Jia and J. F. Wang, "Research review of UAV swarm mission planning method," *Systems Engineering and Electronics*, vol. 43, no. 1, pp. 99–111, 2021.

[3] J. I. Yongnan, T. I. Siying, and L. I. Qing, "Recent development of unmanned aerial vehicle swarms," *Acta Aero nautica et Astronautica Sinica*, vol. 41, no. S1, article 723738, 2020.

[4] L. Liu, D. W. Liu, X. G. Wang et al., "Analysis of the development status of unmanned clusters and anti-unmanned clusters," *Acta Aero-nautica et Astronautica Sinica*, vol. 43, no. S1, article 526908, 2022(in Chinese).

[5] L. Lin, *Research on Multi-UAV Mission Planning Based on Collaborative Mechanism*, Beijing University of Posts and Telecommunications, Beijing, China, 2013.

[6] C. Zhao, Y. Liu, L. Chen, F. Li, and Y. Man, "Research and development trend of multi-UAV path planning based on metaheuristic algorithm," *Control and Decision*, vol. 37, no. 5, pp. 1102–1115, 2022.

[7] N. Wang, Z. Li, X. Liang, Y. Li, and F. Zhao, "Cooperative target search of UAV swarm with communication distance constraint," *Mathematical Problems in Engineering*, vol. 2021, Article ID 3794329, 14 pages, 2021.

[8] Z. Zhen, Y. Chen, L. Wen, and B. Han, "An intelligent cooperative mission planning scheme of UAV swarm in uncertain dynamic environment," *Aerospace Science and Technology*, vol. 100, article 105826, 2020.

[9] T. Huang, D. Huang, N. Qin, and Y. Li, "Path planning and control of a quadrotor UAV based on an improved APF using parallel search," *International Journal of Aerospace Engineering*, vol. 2021, Article ID 5524841, 14 pages, 2021.

[10] J. Tian, *Research on Modeling and Optimization Technology of Multi-UAV Collaborative Detection Mission Planning*, National University of Defense Technology, Changshan, China, 2007.

[11] T. Wang, B. Zhang, M. Zhang, and S. Zhang, "Multi-UAV collaborative path planning method based on attention mechanism," *Mathematical Problems in Engineering*, vol. 2021, Article ID 6964875, 8 pages, 2021.

[12] J. Tian, L. Shen, and Y. Zheng, *Genetic Algorithm Based Approach for Multi-UAV Cooperative Reconnaissance Mission Planning Problem*, Lecture Notes in Computer Science, Springer, Berlin, Heidelberg, 2006.

[13] K. Shi, X. Zhang, and S. Xia, "Multiple swarm fruit fly optimization algorithm based path planning method for multi-UAVs," *Applied Sciences*, vol. 10, no. 8, p. 2822, 2020.

[14] X. Chai, Z. Zheng, J. Xiao et al., "Multi-strategy fusion differential evolution algorithm for UAV path planning in complex environment," *Aerospace Science and Technology*, vol. 121, article 107287, 2022.

[15] D. Qi, Z. Zhang, and Q. Zhang, "Path planning of multirotor UAV based on the improved ant colony algorithm," *Journal of Robotics*, vol. 2022, Article ID 2168964, 9 pages, 2022.

[16] W. Liu and X. Zheng, "Three-dimensional multi-mission planning of UAV using improved ant colony optimization algorithm based on the finite-time constraints," *International Journal of Computational Intelligence Systems*, vol. 14, no. 1, p. 79, 2021.

[17] J.-J. Shin and H. Bang, "UAV Path planning under dynamic threats using an improved PSO algorithm," *International Journal of Aerospace Engineering*, vol. 2020, Article ID 8820284, 17 pages, 2020.

[18] C. Huang, "A novel three-dimensional path planning method for fixed-wing UAV using improved particle swarm optimization algorithm," *International Journal of Aerospace Engineering*, vol. 2021, Article ID 7667173, 19 pages, 2021.

[19] J. Guo, C. Liang, K. Wang, B. Sang, and Y. Wu, "Three-dimensional autonomous obstacle avoidance algorithm for UAV based on circular arc trajectory," *International journal of aerospace engineering*, vol. 2021, Article ID 8819618, 13 pages, 2021.

[20] F. Arab, F. A. Shirazi, and M. R. H. Yazdi, "Planning and distributed control for cooperative transportation of a non- uniform slung-load by multiple quadrotors," *Aerospace Science and Technology*, vol. 117, article 106917, 2021.

[21] Q. Xue, Y. Li, R. Jin et al., "Improved F-RRT * algorithm for flight-path optimization in hazardous weather," *International Journal of Aerospace Engineering*, vol. 2022, Article ID 1166968, 14 pages, 2022.

[22] Y. Guo, X. Liu, X. Liu, Y. Yang, and W. Zhang, "FC-RRT *: an improved path planning algorithm for UAV in 3D complex environment," *ISPRS International Journal of GeoInformation*, vol. 11, no. 2, p. 112, 2022.

[23] F. Yang, X. Fang, F. Gao et al., "Obstacle avoidance path planning for UAV based on improved RRT algorithm," *Discrete Dynamics in Nature and Society*, vol. 2022, Article ID 4544499, 9 pages, 2022.

[24] J. W. Woo, J.-Y. An, M. G. Cho, and C.-J. Kim, "Integration of path planning, trajectory generation and trajectory tracking control for aircraft mission autonomy," *Aerospace Science and Technology*, vol. 118, article 107014, 2021.

[25] Y. Huang, J. Xu, M. Shi, and L. Liang, "Time-efficient coverage path planning for energy-constrained UAV," *Wireless Communications and Mobile Computing*, vol. 2022, Article ID 5905809, 15 pages, 2022.

[26] X. Shao, J. Zhang, and W. Zhang, "Distributed cooperative surrounding control for mobile robots with uncertainties and aperiodic sampling," *IEEE Transactions on Intelligent Transportation Systems*, vol. 23, no. 10, pp. 18951–18961, 2022.

[27] J. Zhang, X. Shao, W. Zhang, and J. Na, "Path-Following Control Capable of Reinforcing Transient Performances for Networked Mobile Robots over a Single Curve," *IEEE Transactions on Instrumentation and Measurement*, p. 1, 2022.

[28] W. Zhang, X. Shao, W. Zhang, J. Qi, and H. Li, "Unknown input observer-based appointed-time funnel control for quadrotors," *Aerospace Science and Technology*, vol. 126, article 107351, 2022.

[29] X. Shao, J. Zhang, X. Lexiu, and W. Zhang, "Appointed-time guaranteed adaptive fault-tolerant attitude tracking for quadrotors with aperiodic data updating," *Aerospace Science and Technology*, no. article 107881, 2022.

[30] R. S. de Moraes and E. P. de Freitas, "Multi-UAV based crowd monitoring system," *IEEE Transactions on Aerospace and Electronic Systems*, vol. 56, no. 2, pp. 1332–1345, 2020.